THE GEOLOGICAL SOCIETY OF AMERICA®

# Probabilistic Seismic Hazard Estimates Incorporating Site Effects—An Example from Indiana, U.S.A.

JENNIFER S. HAASE

*Department of Earth and Atmospheric Sciences, Purdue University, 550 Stadium Mall Drive, West Lafayette, IN 47907-2051*

CHI HYUN PARK

*Schnabel Engineering, 656 Quince Orchard Road, Suite 700, Gaithersburg, MD 20878*

ROBERT L. NOWACK

*Department of Earth and Atmospheric Sciences, Purdue University, 550 Stadium Mall Drive, West Lafayette, IN 47907-2051*

JOHN R. HILL

*Indiana Geological Survey, 611 North Walnut Grove, Bloomington, IN 47405*

**Key Terms:** ***Seismic Hazard, Site Effects***

## ABSTRACT

**The U.S. Geological Survey (USGS) has published probabilistic earthquake hazard maps for the United States based on current knowledge of past earthquake activity and geological constraints on earthquake potential. These maps for the central and eastern United States assume standard site conditions with S-wave velocities of 760 m/s in the top 30 m. For urban and infrastructure planning and long-term budgeting, the public is interested in similar probabilistic seismic hazard maps that take into account near-surface geological materials. We have implemented a probabilistic method for incorporating site effects into the USGS seismic hazard analysis that takes into account the first-order effects of the surface geologic conditions. The thicknesses of sediments, which play a large role in amplification, were derived from a P-wave refraction database with over 13,000 profiles, and a preliminary geology-based velocity model was constructed from available information on S-wave velocities. An interesting feature of the preliminary hazard maps incorporating site effects is the approximate factor of two increases in the 1-Hz spectral acceleration with 2 percent probability of exceedance in 50 years for parts of the greater Indianapolis metropolitan region and surrounding parts of central Indiana. This effect is primarily due to the relatively thick sequence of sediments infilling ancient bedrock topography that has been deposited since the Pleistocene Epoch. As expected, the Late Pleistocene and Holocene depositional systems of the Wabash and Ohio Rivers produce additional amplification in the southwestern part of Indiana. Ground motions decrease, as would be expected, toward the bedrock units in south-central Indiana, where motions are significantly lower than the values on the USGS maps.**

## INTRODUCTION

For the states of Indiana and Illinois in the United States there is a strong gradient in seismic hazard from the south to the north because of the dominance of the New Madrid seismic zone and the Wabash Valley seismic zone in contributing to the hazard (Figure 1). The New Madrid seismic zone produced three events with magnitude greater than $M_w$ 7 during the period ranging from 1811 to 1812. The effects are clear in the seismicity maps of the central United States as well as in the national seismic hazard maps (Figure 2). This presents difficulties for regional seismic hazard assessment efforts when one part of the state is in a stable cratonic region and another is in an active tectonic zone. There is continuing debate on the implications of uncertainties with regard to the maximum magnitude of a repeat of the New Madrid earthquake for the seismic hazard. However, in Indiana, where many sites would fall into National Earthquake Hazards Research Program (NEHRP) site classification D or E (FEMA-222A, 1994), the variations in the expected level of shaking from an earthquake due to variations of near-surface site

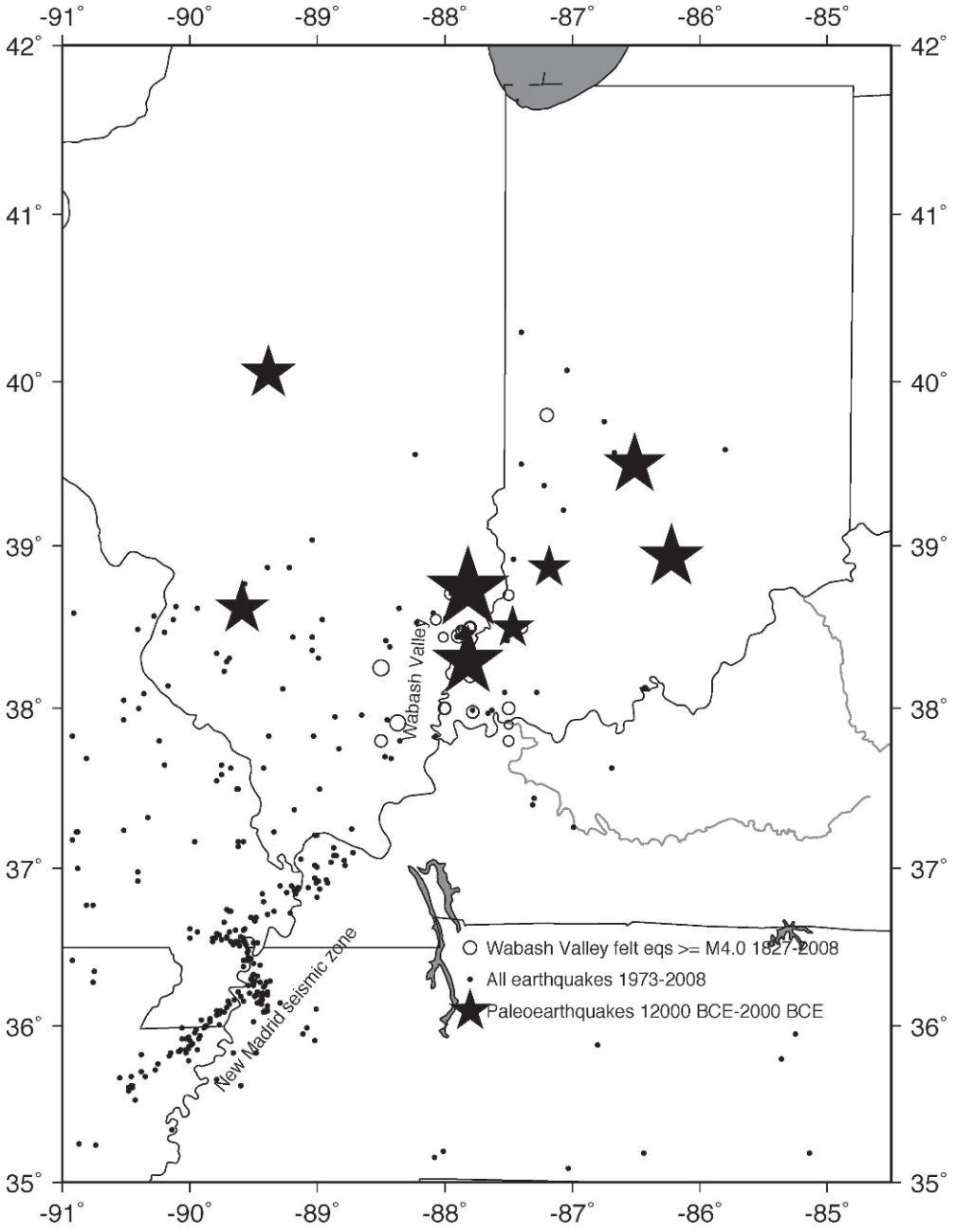


Figure 1. Locations of instrumentally recorded earthquakes greater than or equal to $M_w$ 3.0 from 1973 to 2008 from the National Earthquake Information Center (Sipkin et al., 2000; dots). Historical felt earthquakes (Seeber and Armbruster, 1991; circles) and energy centers from large prehistoric earthquakes from 12000 to 2000 BCE in the southern Illinois basin (Wheeler and Cramer, 2002; stars) are also shown.

conditions are expected to rival the importance of variations due to the uncertainty in the source models for the seismic hazard maps. The goal of this study is to evaluate the importance of variations in near-surface site conditions with regard to seismic hazard estimates for the state of Indiana.

A new methodology has been developed to incorporate soil profile site effects into the probabilistic calculation (Cramer, 2003, 2005). We applied this approach to a low-resolution near-surface velocity model that was derived from a limited amount of seismic refraction and soil profile data in Indiana. This study reports on the relative amplification and de-amplification expected given the available data. The first section reviews the state of knowledge of seismic hazard in the tri-state region, which provides the input to the Probabilistic Seismic Hazard Analysis (PSHA). The second section describes the data sets

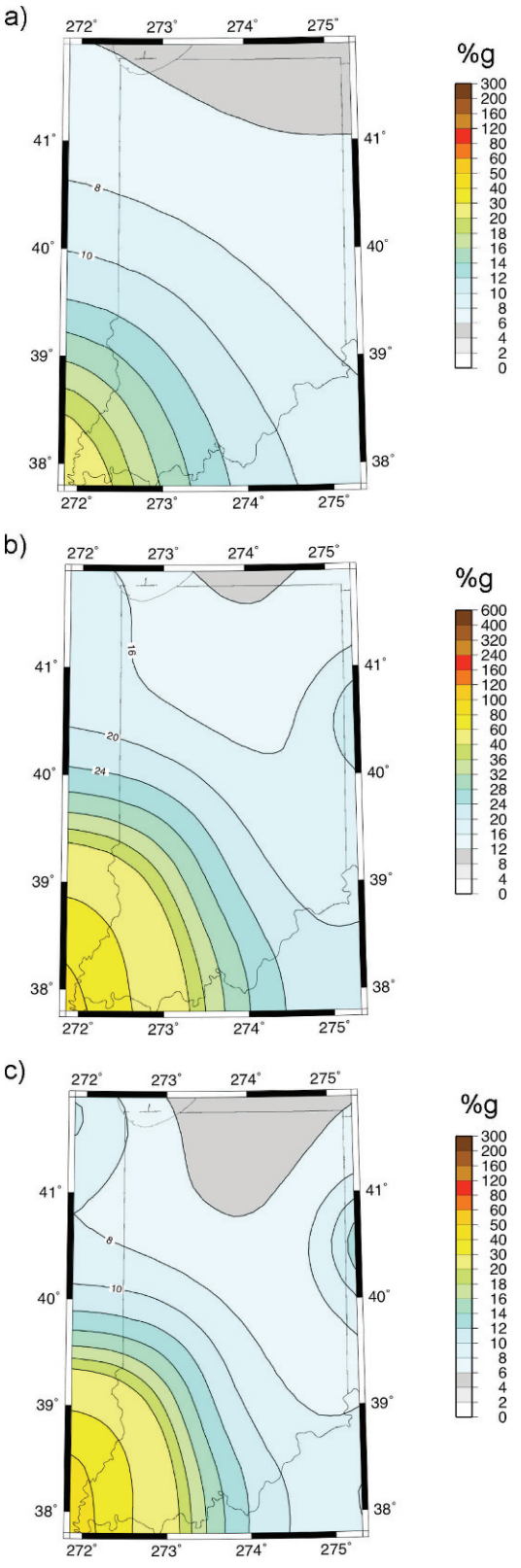


Figure 2. Reproduction of the probabilistic seismic hazard with 2 percent probability of exceedance in 50 years, which includes, by default, the site response for a NEHRP B/C site classification, calculated using the original USGS national seismic hazard mapping method (Frankel et al., 1996, 2002). (a) 1-Hz spectral acceleration (percent g); (b) 5-Hz spectral acceleration (percent g); (c) PGA (percent g).

that were used to establish the input geology–based shear wave velocity model, including comparisons among independent data sets that allow us to estimate the uncertainty of the measurements. The third section summarizes the methodology for the probabilistic calculation and the site response. The fourth section shows the resulting probabilistic seismic hazard maps that incorporate site effects. We then compare the results with the original U.S. Geological Survey (USGS) 2002 maps and comment on the overall increase in acceleration levels.

## SEISMIC HAZARD IN INDIANA

Seismic hazard in the part of the Midwestern United States that includes Indiana is primarily associated with seismicity in the New Madrid seismic zone and the Wabash Valley seismic zone, and to a lower degree with the background seismicity level. Although the dynamics behind the seismic activity are poorly understood, the seismicity itself has been monitored instrumentally since the early 1970s. Seismicity is concentrated in the New Madrid seismic zone, where three major earthquakes occurred in 1811 and 1812. The magnitudes of these events were estimated from intensity reports to be $M_w$ 8.1, 7.8, and 8.0 (Johnston and Schweig, 1996), using a relationship between intensity and magnitude developed for stable continental regions (Johnston, 1996). However, a more recent study (Hough et al., 2000) indicates that the data were biased because they came predominantly from populated regions in river valleys, where motions would be subject to local site amplification. The study of Hough et al. (2000) revises the magnitudes to $M_w$ 7.2–7.3, 7.0, and 7.4–7.5. The events are presumed to have occurred on the 200-km–long segmented fault system that is delineated by current seismicity along and to the north of the axis of the Reelfoot Rift. Although the Reelfoot Rift formed during a stage of rifting in the Late Proterozoic to Cambrian, it is believed that the rift faults have been re-activated in the modern stress field with an east-northeast trending maximum horizontal compressive stress (Zoback and Zoback, 1991). The evidence for an ancient failed rift in the mid-continent lies in the presence of strong gravity and magnetic anomalies indicating mafic material at subcrustal depths beneath the Mississippi embayment (Braile et al., 1982). Deep seismic reflection and refraction surveys place strong reflectors at depths of greater

than 15 km. These anomalies have been interpreted as a rift system and possible triple junction that started forming during the Late Pre-Cambrian to Middle Cambrian time period. Different authors have postulated that current seismicity may be preferentially located at rheological boundaries at the edge of the mafic units in the ancient rift zone, where stress may be concentrated, or that pre-existing zones of weakness are re-activated as strike-slip faults under present plate boundary forces. Some work (Zoback, 1992) has indicated that glacial rebound contributes to variations in the stress field that produce seismicity. There is evidence from gravity and magnetic anomalies that branches of this rift extend northeast into Indiana and west beneath the Illinois basin (Braile et al., 1982). Paleoliquefaction studies have indicated that earthquakes similar to the 1811–1812 earthquake sequence have occurred in about AD 1500 and 900, implying a recurrence interval of 500 ± 100 years for large events (Tuttle and Schweig, 1995; Kelson et al., 1996; and Tuttle et al., 1999).

There is significant seismicity in the Illinois basin, which has a background rate that implies that the region is capable of producing magnitude-5 earthquakes on the order of every 10 years. There is historic evidence for large earthquakes in the southern Illinois basin region, which includes the Wabash Valley fault zone, where at least eight earthquakes large enough to cause liquefaction occurred during the Holocene and Pleistocene periods. The largest two earthquakes had estimated moment magnitudes of $M_w$ 7.5 (for the Vincennes earthquake, at approximately 6100 before present [BP] [Green et al., 2005]) and $M_w$ 6.7 (for the Skelton–Mt Carmel earthquake, at approximately 12000 BP [Olson et al., 2005]). There is not sufficient evidence to attribute these earthquakes to a specific fault and to estimate a recurrence interval. The occurrence of the events, however, does motivate a larger maximum magnitude of 7.5 in the extended Wabash Valley seismic zone in the probabilistic seismic hazard calculations than in surrounding regions of Illinois and Indiana (Wheeler and Cramer, 2002).

The 2002 USGS probabilistic seismic hazard estimates (Frankel et al., 2002) show a higher seismic hazard in southwestern Indiana than for the rest of the state. However, the expected level of shaking is likely to differ significantly, because local soil conditions can produce amplification of shaking in regions with surface sediments relative to firm-rock sites. Indiana predominantly has sites with D- and E-level NEHRP classifications. We have reproduced the probabilistic seismic hazard calculation following the USGS methodology for the state of Indiana (Figure 2). The probabilistic maps were constructed assuming firm-rock sites with shear wave velocities corresponding to the NEHRP B/C classification boundary. Versions of the maps were produced for other NEHRP classification levels; however, no information was provided specific to the state of Indiana that indicates which site classification is appropriate for a given location. More recent studies have attempted to provide more detailed soil amplification classifications for the central United States. These are described by Bauer et al. (2001) and Street et al. (2001).

Previous estimates of probabilistic seismic hazard (Toro and Silva, 2001; Frankel et al., 2002) made a simple assumption that the acceleration levels in the probabilistic seismic hazard maps can be multiplied by the relevant amplification factor to incorporate site effects. However, this does not take into account the uncertainties in the knowledge of the amplification factor, which has been shown in some cases to make a difference of 0.1 g or greater (Cramer, 2003). For a completely probabilistic treatment of the ground motions, several methods have been proposed (Lee, 2000; Toro and Silva, 2001; Bechtel-Jacobs, 2002; and Cramer, 2003) to incorporate the uncertainties in the soil profile by modifying the attenuation curve appropriately within the probabilistic seismic hazard calculation directly. This is the approach we use in this article.

## DATA AND INPUT SHEAR WAVE VELOCITY MODEL

Estimates of the shear wave velocity profiles and dynamic properties at each point in the map area and their associated uncertainties are required to implement a probabilistic calculation that incorporates site information. This is not directly available at the 0.05-degree resolution of the national seismic hazard maps. Though some direct measurements are available, it is necessary to extrapolate the available information to the entire region of interest in a logical manner based on the available geological data. In a study of the Memphis area Gomberg et al. (2003) were able to uniquely classify five lithologic units, reaching depths of approximately 30 m. This was possible because of the dense subsurface sampling (1,200 geophysical well logs and 76 velocity profiles) within a limited 45 by 25–km area. The depositional environment of the Mississippi embayment is relatively simple in the Memphis area, so that layers are nearly continuous and can be correlated over the entire map area. Because of the low density of available data for the extended area of this study, we necessarily use a simplified method to derive a velocity model. We use the data described below to

infer a gridded model of shear wave velocity for a single layer of unconsolidated soil over bedrock on a 0.125-degree grid, where that layer has the average properties of the soils predominantly found in that quadrangle, rather than the exact structural geometry of a particular layer unit.

## Geologic Data

The bedrock geology of Indiana consists of gently eastward-dipping sequences of shales, limestones, and sandstones of Paleozoic age formed from material deposited when transgressing shallow seas covered most of the North American continent (Figure 3). These bedrock units are covered by unconsolidated deposits left from several intervals of glaciation in the Tertiary and Quaternary periods. Glacial tills from both northern and northeastern sources overlap in a complicated sequence, along with associated glacial outwash deposits, wind-blown glacial loess, and some sand and silt deposits from shallow glacial and post-glacial lakes. Bedrock is exposed at the surface over a large part of south-central Indiana, south of the limit of the Wisconsinian and older stages of glaciation, which corresponds approximately to the limit of the loam till unit shown in Figure 4. This 1:500,000 scale quaternary geologic map (Gray, 1989) shows 34 different surficial units distinguished by lithology and depositional environment. Significant thicknesses of alluvial deposits are found in the Wabash and Ohio River valleys near the southern and southeastern borders of the state. We group these thicknesses into six general types of materials—alluvium, eolian sand, loess, outwash deposits, lacustrine deposits, and glacial tills—in order to create a simplified surficial geologic map (Figure 5).

## Seismic Data

The six general types of material are each assigned a shear wave velocity based on the available data (Hill and Foshee, 2008). Borehole shear wave velocity measurements are available in the Evansville and Vincennes region (Eggert et al., 1994). These are primarily in the glacial outwash and alluvial sequences that are found in the Ohio River valley (Eggert et al., 1997). The maximum depth of the boreholes is 40 m, with many reaching bedrock. Shear wave velocities can be up to 600 m/s in these soils. These data were used to create a site classification map based on geology and the average shear wave velocity in the upper 30 m (Bauer, 1997), using the NEHRP site classifications (FEMA-222A, 1994). In order to characterize other major units present in Indiana, additional borehole velocity measurements were made by the Indiana Geological Survey in the summer of 2003 (Hill and Foshee, 2008). For each material type, the available data were averaged to derive a mean shear wave velocity and standard deviation. The derived values are shown in Table 1. Units containing primarily sand typically have higher velocities than finer-grained materials, as expected (Hamilton, 1979), and the highest soil velocities are found in the glacial tills.

We created a grid using the center points of the USGS topographic map quadrangles with 0.125-degree spacing. Each grid point was assigned the average shear wave velocity from Table 1 corresponding to the geologic unit within which the grid point falls (Figure 6). Shear wave velocities for grid points where bedrock is mapped at the surface are assigned a 760-m/s firm-rock velocity. The presence of weathered residuum on the outcropping bedrock requires the use of slower velocities than those compiled for similar pristine Illinois bedrock units (Bauer et al., 2001). We adopted dynamic properties of soil damping ratio and modulus reduction curves from standard curves associated with similar soil types (Table 1) (Rockaway, 1997).

Seismic refraction data were used to constrain the soil depth and the underlying bedrock velocities. Over 13,000 refraction measurements of compressional wave velocity were made between the years 1954 and 1973 (Rudman et al., 1973; Whaley et al., 2002). Seismic P-wave velocities for bedrock were determined for each profile, as were velocities for a maximum of three soil layers, along with the soil layer thicknesses. Shear wave velocity cannot be reliably related to compressional wave velocity in the soils, especially near the surface; however, the bedrock shear wave velocities can be inferred from the compressional velocity by dividing by the theoretical Vp:Vs ratio of 1.73 for a Poisson solid. We assume the P-wave layer interface depths can be used to approximate the S-wave velocity layer interface depths for the soil layers.

The refraction measurements were first screened to remove data of lower quality. This reduced the data set to 11,873 profiles (Figure 7). Then the bedrock velocities within each 0.125 by 0.125–degree quadrangle were averaged to derive a mean velocity and standard deviation. Typically, most quadrangles contained at least four measurements. For quadrangles with less than two measurements, the average bedrock velocity from the nearest quadrangle with data was assigned. The average velocity is closely correlated with bedrock type (Figures 3 and 8). The values for each quadrangle were divided by 1.73 to obtain the average shear wave velocity and standard deviation.

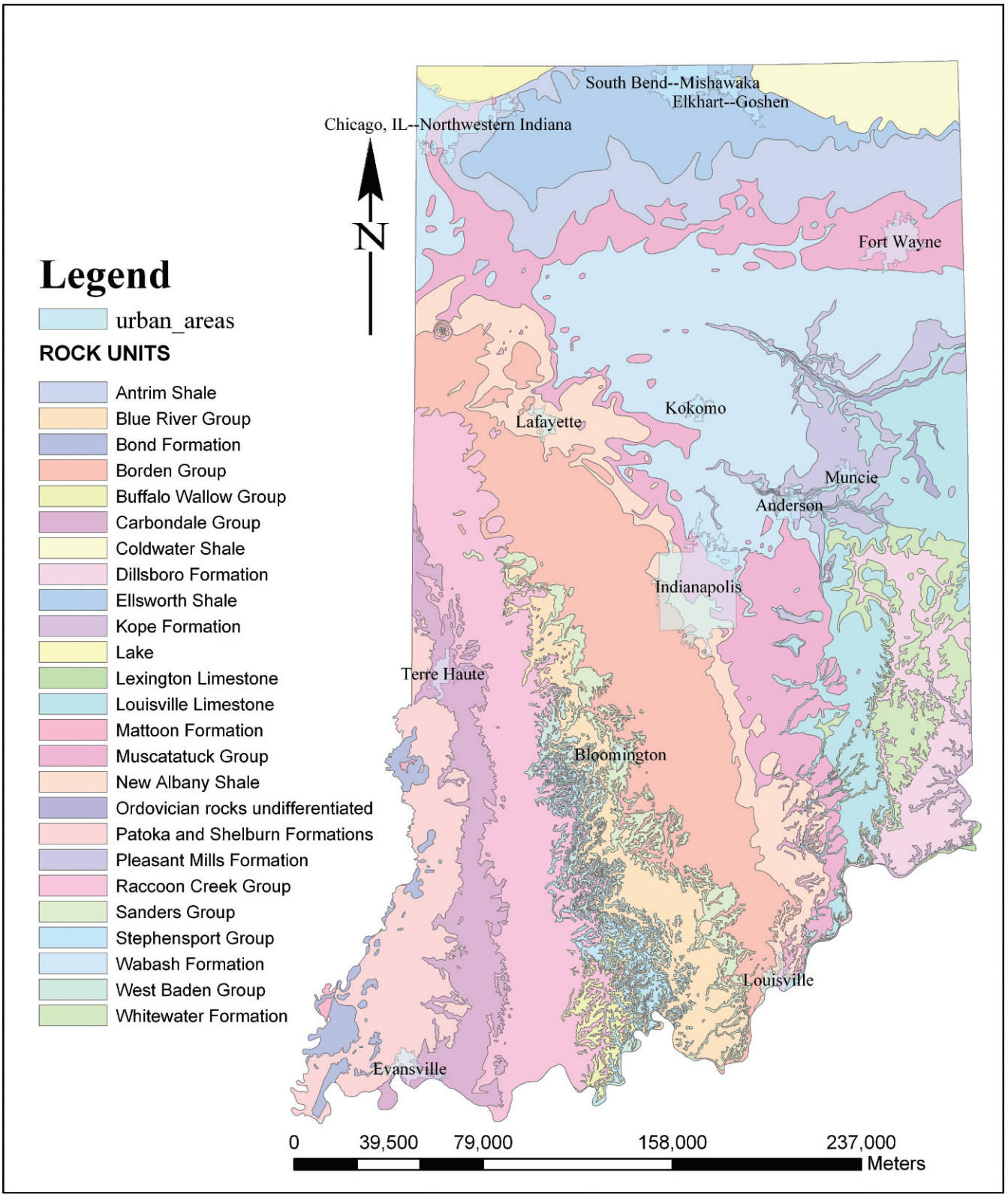


Figure 3. Bedrock geology map of Indiana (Gray, 1989).

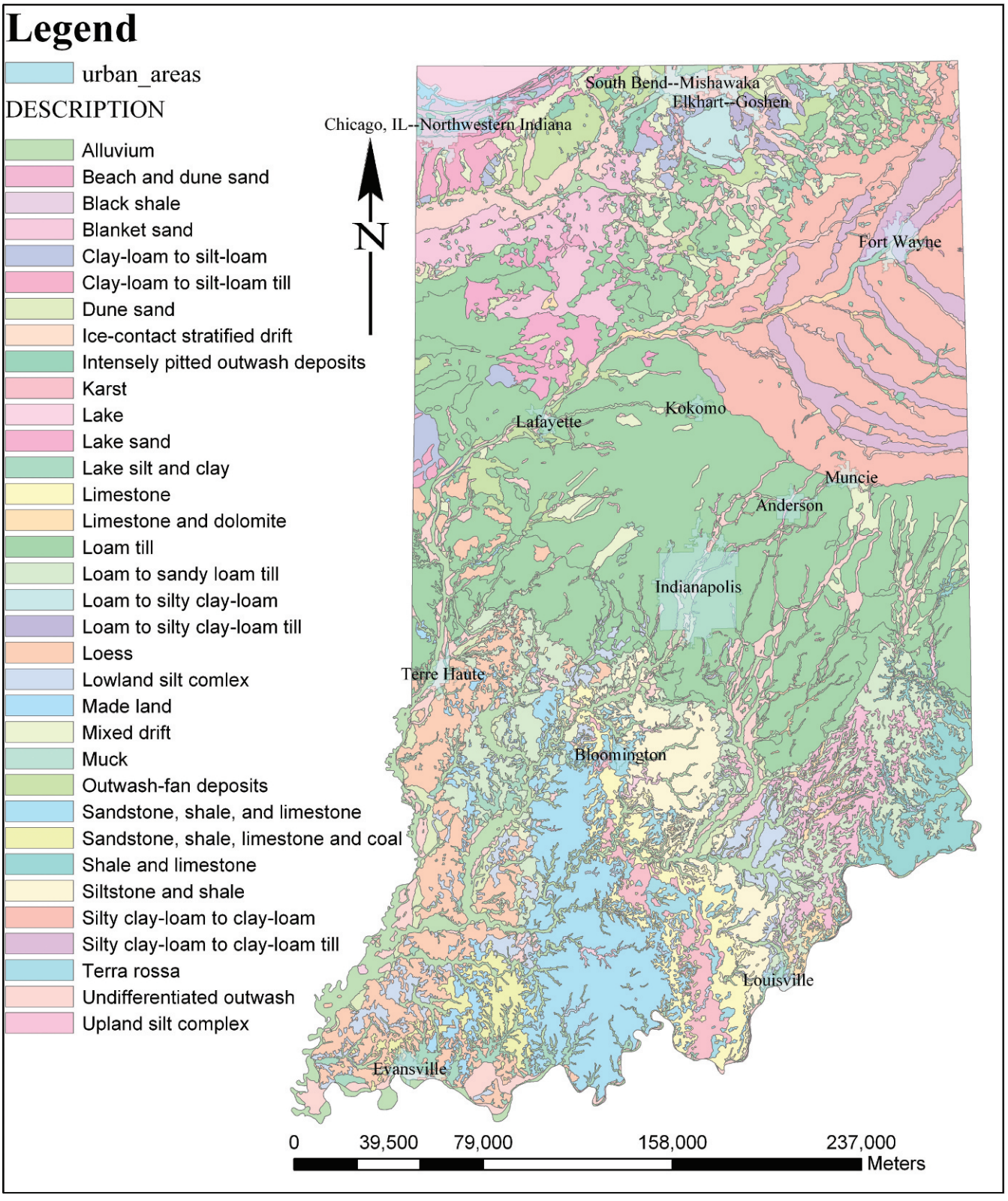


Figure 4. Surficial geology map of Indiana (Gray, 1989).

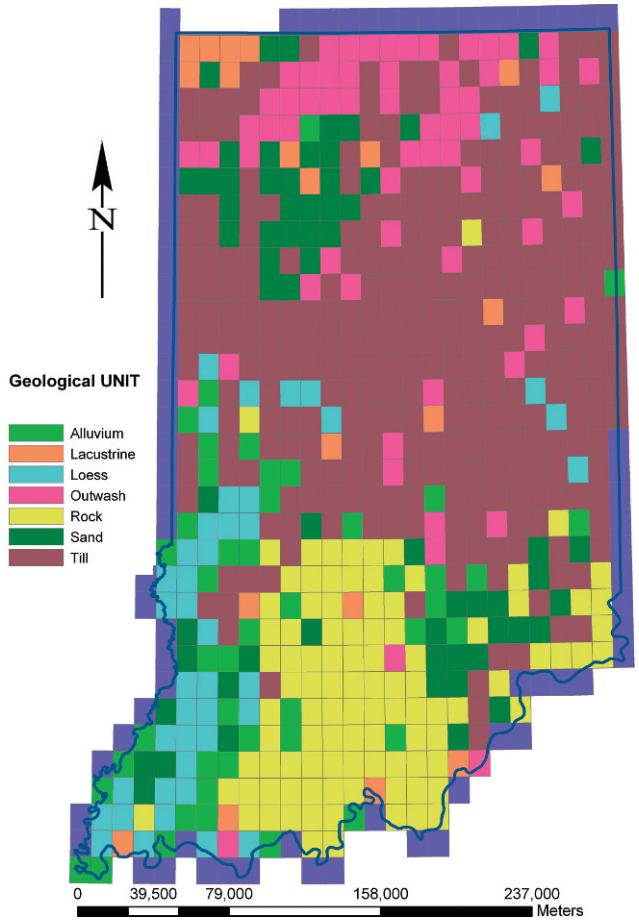


Figure 5. Surficial material type map, simplified from the surficial geology map. The original surficial geologic units have been grouped by material type, given in Table 1.

The average thickness of the soils is derived from the seismic refraction data within each quadrangle. The individual P-wave profiles typically have one or two soil layers over bedrock. Soil layer 1, when present, is often less than 5 m thick, and P-wave velocities in this layer do not correlate with large-scale surficial geology. However, the P-wave velocities in soil layer 2 (Figure 9a) correlate strongly with total thickness of the soil column (depth to the base of soil layer 2; Figure 9b) and with the surficial geology (Figure 4). Though Poisson's ratio cannot be used to estimate S-wave velocity from P-wave velocity, the correlation of the soil layer 2 P-wave velocity with surficial geologic unit type provides support for assigning S-wave velocity based on characteristic S-wave velocities made at a few points in each surficial geologic unit type. A single average velocity was assigned to the soil column above bedrock, and the depths of individual interfaces were retained, so that in the randomization process used in the amplification calculation, some velocity contrast at these interfaces would be allowed. The depths to the base of soil layer 1 and depths to the base of soil layer 2 (bedrock depth) were averaged for each quadrangle, and the standard deviation was calculated. For quadrangles for which there were no profiles available, the bedrock depth from the nearest quadrangle with data was used. The standard deviation of the depths is on the order of 20 percent for most quadrangles, so this value was used in the randomization process for generating the amplification statistics. The bedrock depth is consistent with an older interpreted map of the bedrock depth for Indiana (Gray, 1983), based on seismic refraction data and water well data.

The methodology that we have adopted for determining an S-wave velocity model is limited in resolution, given the true geological complexity of the state. In the future one would hope to make many more direct measurements of seismic velocity in each of the units to reduce the uncertainty for each classification and also to allow for a more complicated representation of the soils with depth. However, as long as the uncertainty for each of the parameters is estimated correctly, the uncertainties in the final seismic hazard estimates are adequately represented.

## PROBABILISTIC HAZARD METHODOLOGY

The methodology used to create a probabilistic hazard map that includes site effects is based on the

Table 1. *Column shear wave velocity (V) averaged by unit type from borehole velocity measurements. Values assigned for specific gravity were taken from Rockaway (1997).*

| Unit Type | Average Vs (m/s) | SD Vs (m/s) | Specific Gravity | Shear Modulus Reduction Curve | Soil Damping Ratio |
|---|---|---|---|---|---|
| Alluvial | 256 | 41 | 1.92 | Average gravel (Seed et al., 1986) | Average gravel (Seed et al., 1986) |
| Eolian sand or sand | 249 | 59 | 1.76 | EPRI generic sand | EPRI generic sand |
| Lacustrine | 202 | 31 | 1.92 | Clay (Sun et al., 1988) | Clay (Vucetic and Dobry, 1991) |
| Loess | 208 | 40 | 1.84 | Clay (Sun et al., 1988) | EPRI generic sand |
| Outwash | 230 | 18 | 1.92 | Average gravel (Seed et al., 1986) | Average gravel (Seed et al., 1986) |
| Till | 350 | 34 | 1.92 | Average gravel (Seed et al., 1986) | Average gravel (Seed et al., 1986) |
| Rock | — | — | 2.4 | EPRI generic rock | EPRI generic rock |

SD = standard deviation.

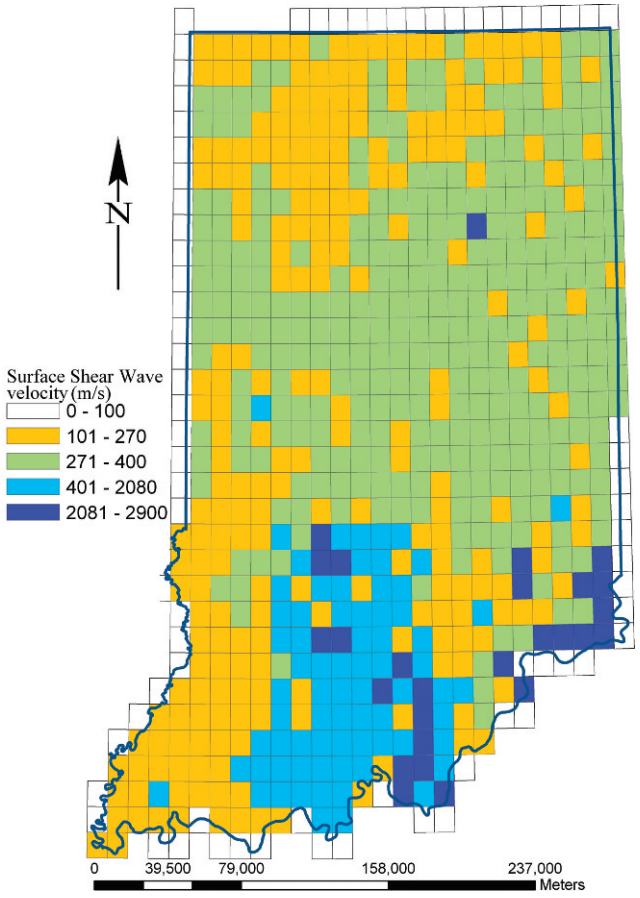


Figure 6. Surface shear wave velocity map, with velocity assigned to the unit type as shown in Table 1.

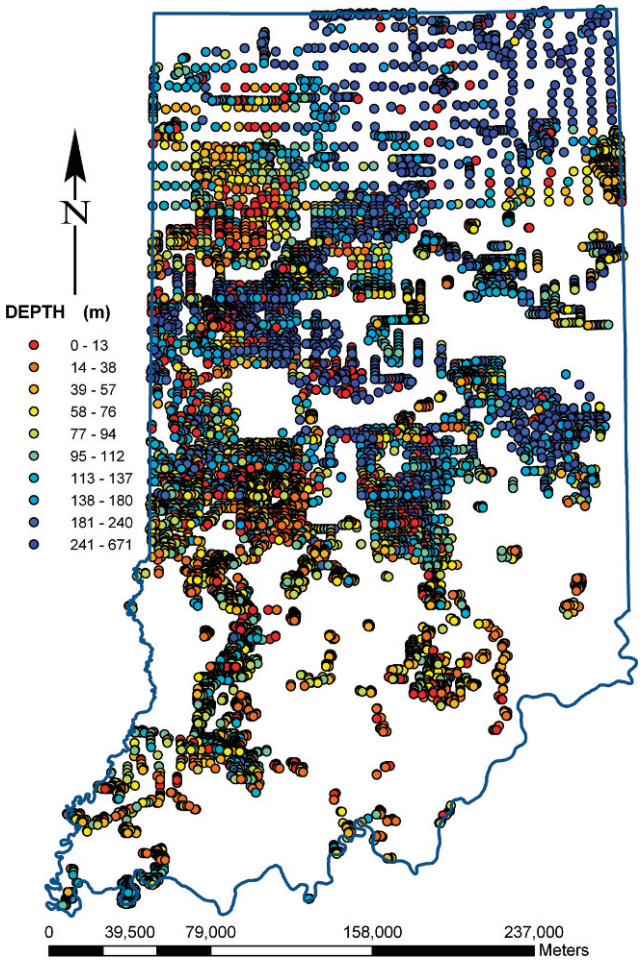


Figure 7. Map of locations of 11,873 P-wave refraction profiles and 28 borehole S-wave velocity profiles.

USGS probabilistic seismic hazard calculation method (Frankel et al., 1996, 2002). The USGS national seismic hazard maps show the hazard in terms of the level of horizontal ground shaking with a specified probability of being exceeded in a given time period for NEHRP B/C site conditions, with an assumed S-wave velocity of 760 m/s. For reference, we have reproduced this calculation for the study area (Figure 2).

We extend this calculation to include site effects using the methodology suggested by Cramer (2003). For a given site, the probability, $P$, of exceeding a specific ground motion, $A_0$ (Reiter, 1990), is the sum of the probability of exceeding that ground motion level for all possible source earthquakes:

$$P(A_r > A_0) = \sum_i \alpha_i \int_M \int_R f_i(M) g_i(R) P(A_r > A_0 | M,R) dR\, dM \quad (1)$$

where $A_r$ is the ground motion parameter (i.e., peak ground acceleration or spectral acceleration) observed at a rock site, $\alpha_i$ is the annual rate of occurrence of the $i$th earthquake source, $f_i(M)$ is the probability density distribution of earthquake magnitude $M$ of the $i$th source, and $g_i(R)$ is the probability density distribution of distance $R$ from the $i$th source. $P(A_r > A_0|M, R)$ is the probability of exceeding ground motion $A_0$, given an earthquake of magnitude $M$ at distance $R$, and is given by an attenuation relation with a log-normal distribution. The latter probability is variable if site effects are incorporated into the calculations. The probability of ground motion at a soil site, $A_s$, exceeding a specific ground motion, $A_0$ (Cramer, 2003), is given by

$$P(A_s > A_0 | M,R) = 1 - \int_{A_x=-\infty}^{A_0} \int_{A_y} P(A_s = A|A_r) P(A_r|M,R) dA_r dA \quad (2)$$

where $P(A_s = A|A_r)$ is the probability of the soil ground motion $A_s = A$, given an input ground motion $A_r$ to the base of the soil column.

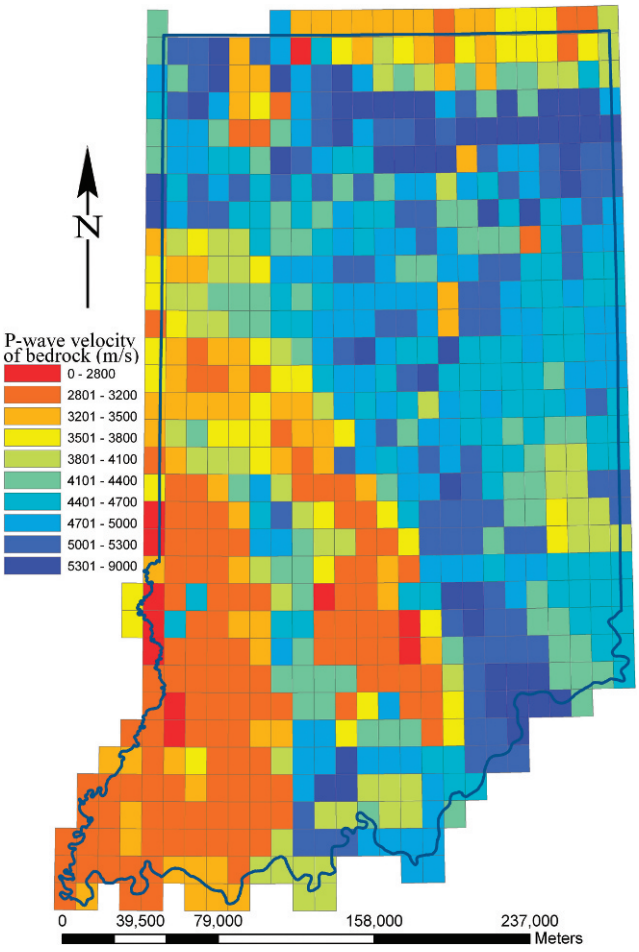


Figure 8. Average bedrock P-wave velocity for each 0.125-degree quadrangle. Note the strong correlation between seismic velocity and bedrock type in Figure 3.

## Site Amplification Calculation

The ground motion at the surface of a soil column, given an input ground motion at the base, is calculated using the program SHAKE91 (Idriss and Sun, 1992). This program uses a frequency domain approach to calculate the transfer function of motions at consecutive layer interfaces. It assumes vertically propagating shear waves that can be approximated as a sum of sine waves. The transfer function depends on the complex shear modulus (shear wave velocity, specific gravity, and soil damping ratio) of the layers and the thickness of the layers. It takes into account non-linear and inelastic behavior of the soil (changes in the shear modulus of the soil depending on the amplitude of the strain) using an iterative equivalent linear approach. This requires estimates of the modulus reduction curve for the soil type. Typically, the transfer function for a stack of low–shear wave velocity soil layers produces an amplification of ground motion. Including non-linear behavior has the effect that for very large ground motions, the amplification due to the soil layers is reduced, or can even be de-amplified. The soil damping ratio describes the viscous attenuation of the amplitude of the seismic waves and has also been characterized for many soil types. In summary, if the shear wave velocity, specific gravity, soil damping ratio, and modulus reduction curves are known for each layer of soil above bedrock, the response of the soil layers can be computed with SHAKE91.

For seismic hazard mapping, as opposed to site-specific studies, one is working at a scale at which the geologic structure is approximated from a limited amount of borehole data with limited accuracy. For this reason, we have characterized the uncertainties in these parameters, as described in the data section above. These uncertainties were used to calculate empirically the probability distribution function required in Eq. 2.

A distribution of site amplification factors was calculated at each 0.125-degree grid point in the study region in the following manner. One hundred realizations of the soil profile were generated that have the distribution of shear wave velocities found for that geologic unit type and the distribution of soil layer thicknesses that were found in the measured refraction profiles at or near that grid point. Generic values for the dynamic soil properties were assumed to be those represented by the Electric Power Research Institute (EPRI, 1993) for sandy soils, depending on the depth range, and by Vucetic and Dobry (1991) for clay soils, chosen based on a study of similar soils (Rockaway, 1997). Variations were introduced in these average modulus reduction curves and damping curves with a natural log-normal standard deviation of 0.35 (EPRI, 1993). Variation is introduced into the scaled input bedrock ground motions by selecting randomly from a set of six ground motions for $M_w$ ~7 earthquakes recorded at firm-rock sites for each realization (Table 2). The six input ground motion recordings came from the PEER strong ground motion database (Pacific Earthquake Engineering Research Center, 2009). The 100 soil profiles were used as input to the site response calculation to create a distribution of site amplification factors at each grid cell for varying levels of input ground motion at the bedrock interface. For each frequency of interest, the site response was computed using input ground motions scaled from 0.01 to 1 g in response to spectral amplitude for the particular frequency of interest (peak ground acceleration [PGA], 5-Hz spectral acceleration, 1-Hz spectral acceleration) to obtain the output amplification. There was no approximation made to scale a PGA value using a standard response spectral shape, which would require further corrections that are not needed if the

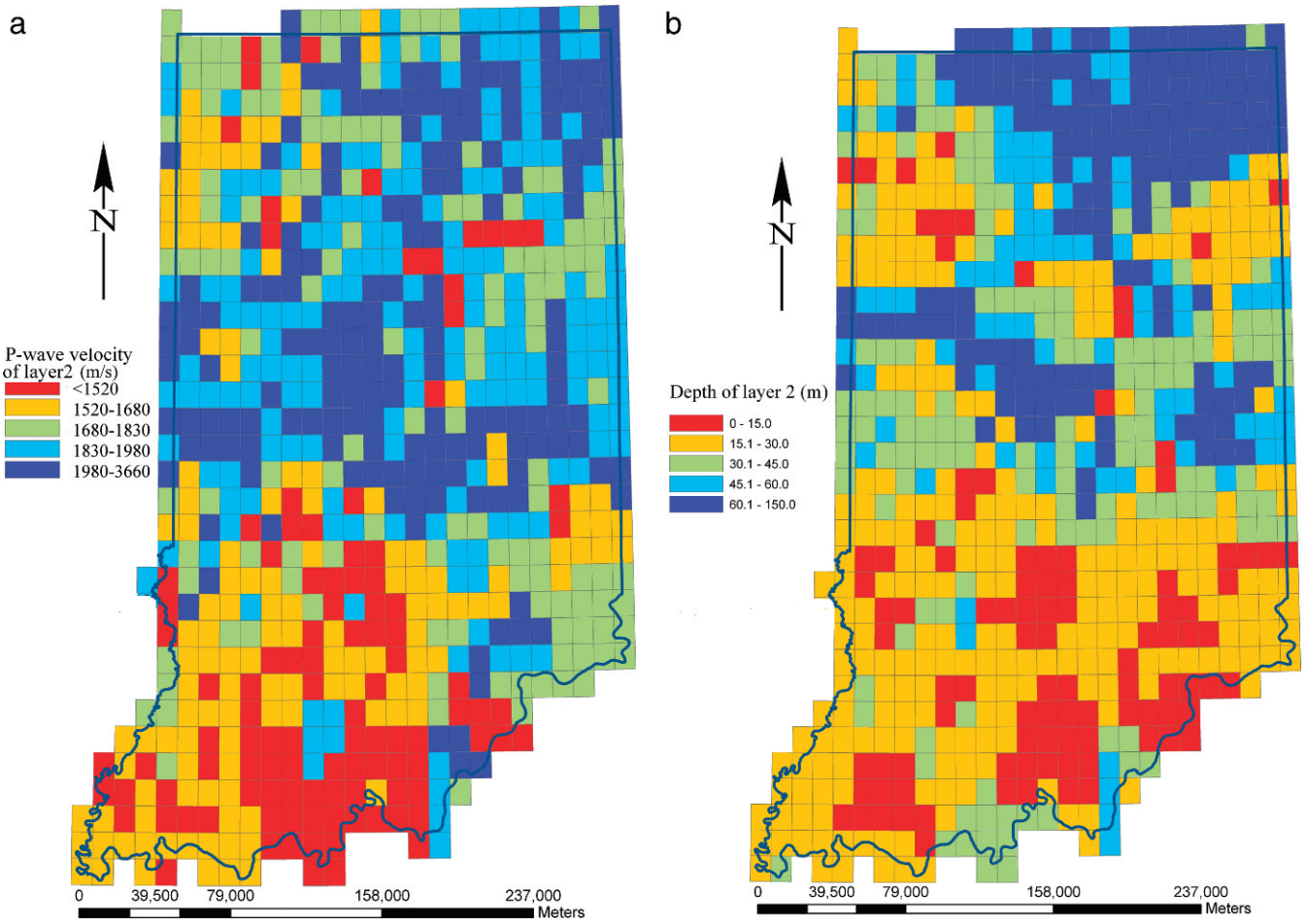


Figure 9. (a) Average P-wave velocity of soil layer 2 in each 0.125-degree quadrangle and (b) depth to the base of soil layer 2 (bedrock depth). P-wave velocity shows a strong correlation with surficial geology. Note the correlation between depth and average P-wave velocity, which indicates that velocity is also a function of effective stress. When present, soil layer 1 is typically less than 5 m deep and does not show a correlation with surface geology.

response is scaled directly at the frequency of interest. The median and log-normal standard deviation of the amplification factors were tabulated for each input ground motion level.

## Hazard Calculation

We then incorporated the probabilistic site amplification into the seismic hazard calculation following the general method for PSHA (Cornell, 1968; Reiter, 1990; and McGuire, 2004), as implemented in the 2002 USGS national seismic hazard maps (Frankel et al., 1996, 2002). Earthquakes from all possible regional seismic sources, each with a given probability of occurrence, were taken into account for this analysis. This included gridded seismic sources estimated from the Gutenberg-Richter relation, valid for observed regional background seismicity, as well as characteristic earthquake sources along known faults with estimated recurrence rates. The seismicity-derived hazard component was based on a catalog of central and eastern United States earthquakes with magnitude 3.0 or greater from 1700 through 2001. The size of the largest expected earth-

Table 2. *Suite of input bedrock ground motions used in site response calculation.*

| Event | Date | $M_w$ | Site | Components* |
|---|---|---|---|---|
| Cape Mendocino | April 25, 1992 | 7.0 | CDMG 89005 Cape Mendocino | N, E |
| Kobe | January 16, 1995 | 6.9 | KJMA | N, E |
| Landers | June 28, 1992 | 7.3 | JOS Joshua Tree | N, E |

*N = North, E = East.

quake was $M_w$ 7.0 within the central and eastern parts of the North American continent, away from specific seismic zones, and $M_w$ 7.5 for the extended continental margin. The Wabash Valley region was assigned a maximum magnitude of $M_w$ 7.5 based on paleoliquefaction evidence in the extended Illinois basin (Wheeler and Cramer, 2002). The characteristic earthquake-derived component of the seismic hazard in the central and eastern United States was based on finite source areas, where paleoseismic data constrain recurrence rates in New Madrid, Missouri, and Charleston, South Carolina. Because of the epistemic uncertainty in recurrence rates and earthquake magnitude, several weighted estimates of the seismic hazard were combined using a logic tree approach for varying the different source parameters. Several cases were considered for the most important source region in New Madrid. The seismic source was varied from $M_w$ 7.3 to $M_w$ 8.0, with a recurrence interval of 500 years, and the location of the rupture was varied among three possible locations of the three fault branches that ruptured in 1811 and 1812 (Tuttle et al., 2002).

For each possible earthquake source location and magnitude determined by the source model, the probability of a given ground motion occurring was calculated based on a suite of central and eastern United States seismic attenuation relations (Atkinson and Boore, 1995; Frankel et al., 1996; Toro et al., 1997; Somerville et al., 2001; and Campbell, 2003). The five attenuation relations were derived for, or had been adjusted to, standard NEHRP B/C site conditions (BSSC, 2004), which implies shear wave velocities of 760 m/s in the top 30 m of the soil at a given site. In the probabilistic site effect hazard calculation, the attenuation relations were modified based on the amplification factor distribution at each site to provide new attenuation relations valid for the soil site with modified uncertainties. These modified attenuation relations were used in the probability calculations of ground shaking for the complete range of possible source regions to create the hazard curve describing the annual probability of exceedance of ground motions at a given site in the grid. The ground motions corresponding to a prescribed level of exceedance were selected from the hazard curves at all sites in the region to make a probabilistic hazard map. Further details on the PSHA methodology can be found in the documentation for the national seismic hazard maps and other literature (Cornell, 1968; Reiter, 1990; Frankel et al., 1996, 2002; and McGuire, 2004).

## RESULTS

The results from the first phase of the calculation are the amplification factors for each point of the grid for input ground motions from 0.05 to 1.00 g and their probability density function. The site response amplification as a function of frequency is different depending on the input ground motion level, because the shear modulus reduction curves reduce the amplification at higher strains. For example, at some sites the amplification at 5 Hz may be a factor of 3 for input ground motions of .05 g, but for input ground motions of 0.5 g, the amplification at 5 Hz may only be a factor of 1.4. Contour maps of the amplification for input motions of 0.05 g, 0.2 g, and 0.5 g are shown in Figure 10. The figure for amplification at 1 Hz illustrates the amplification of thicker sediment sequences in the central and northeastern parts of the state. These maps give a preliminary indication of the effect that the site geology will have on the final calculation. One can observe that regions that are not amplified at 1 Hz are preferentially amplified at higher frequencies (5 Hz and PGA), because of the sensitivity of the dominant resonant frequency to different soil thicknesses.

The results of the second phase of the calculation are the ground motions for a given probability level. For this work we ran the calculation for a probability level of 2 percent. The map of 1-Hz spectral acceleration with 2 percent probability of exceedance in 50 years, including the probabilistically determined site response, is shown in Figure 11a. Comparison with the USGS PSHA map (Figure 2), which assumes a NEHRP B/C site classification, shows that there is high amplification of ground motions in several areas of the state. There is a general trend of decreasing accelerations with distance from the primary source regions of the Wabash Valley and New Madrid that is seen in the USGS PSHA maps. However, this trend has been partially obscured by significant smaller-scale variations in acceleration. There is an extensive region of higher accelerations on the order of 0.2 g running northwest to southeast across the center of the state. This region corresponds to the location of the subsurface Teays Valley, a low in the buried relic bedrock topography that was formed by the impoundment of the drainage system by Early Pleistocene glaciation. The valley is filled with a thick sequence of Plio-Pleistocene glacial till. There is another smaller region of relatively higher accelerations in the north of the state and several isolated locations east of the outcropping limestone and shale bedrock in the southern half of the state.

The map of 5-Hz spectral acceleration with 2 percent probability of exceedance in 50 years is shown in Figure 11b. The pattern of accelerations is very different from both the 1-Hz maps and the USGS PSHA maps outside the southwestern corner of the state. The regions of high acceleration tend to lie in between the regions with high 1-Hz spectral accelera-

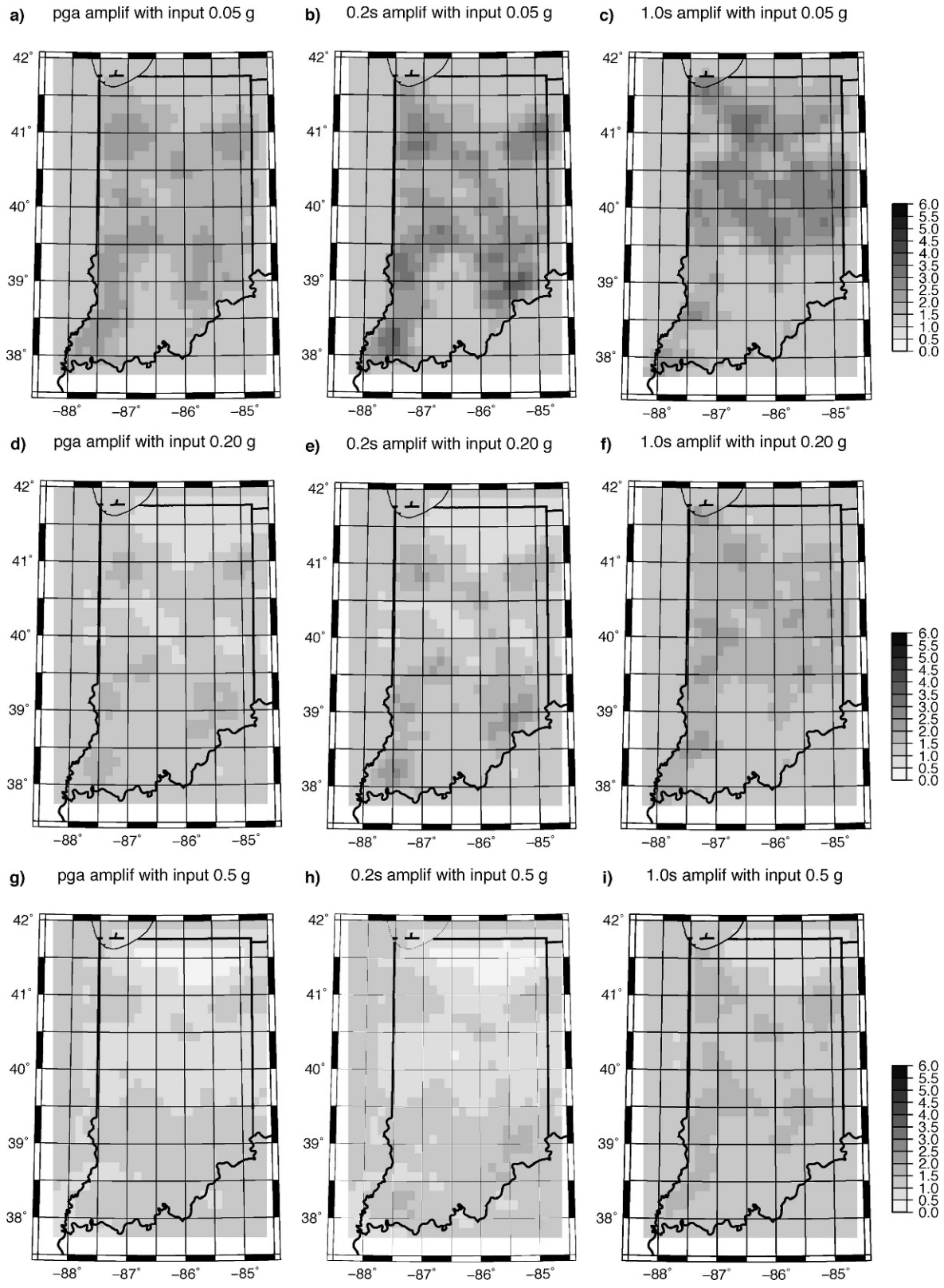


Figure 10. Maps of amplification factor for input ground motion levels of 0.05 g for (a) PGA, (b) 0.2-second spectral acceleration (SA), and (c) 1.0-second SA. Maps for input ground motion levels of 0.20 g for (d) PGA, (e) 0.2-second SA, and (f) 1.0-second SA. Maps for input ground motion levels of 0.50 g for (g) PGA, (h) 0.2-second SA, and (i) 1.0-second SA.

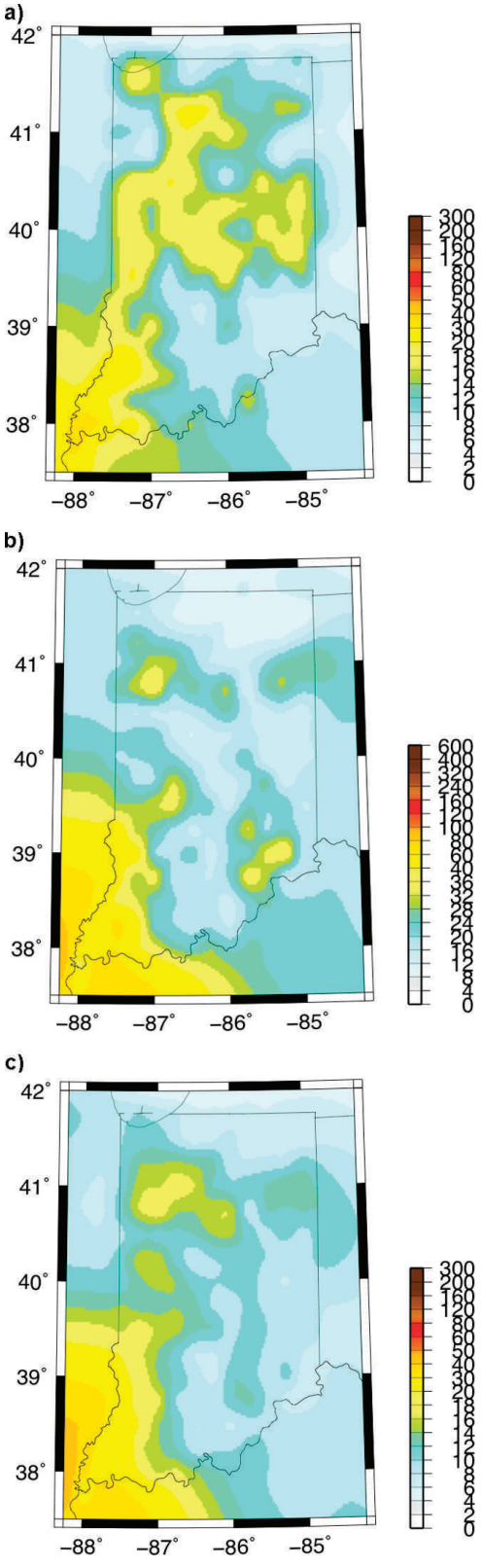


Figure 11. Map of the probabilistic seismic hazard with 2 percent probability of exceedance in 50 years, including the probabilistically determined site response. (a) 1-Hz spectral acceleration (percent g), (b) 5-Hz spectral acceleration (percent g), and (c) PGA (percent g). Note the high amplification of ground motions in the center and northeastern parts of the state at 1 Hz due primarily to the extensive soil thickness.

tion. There is much less significant amplification in the PGA maps. In all maps there are lower accelerations in the bedrock in the south-central portion relative to surrounding areas. As a check on the reasonableness of the results, we compare the probabilistic maps to a simple estimate of the expected resonant period of the surface unconsolidated soil layer. The resonant period at each grid point was calculated as $T = 4h/V_s$, where $h$ is the thickness of the sediments and $V_s$ is the average S-wave velocity of the soil. The map of resonant period (Figure 12) shows that higher amplitudes at specific frequencies do indeed tend to occur where the surface geology is expected to produce a resonance.

Cases have been investigated in which significant differences in the probabilistic hazard estimates are produced by incorporating site effects in a non-probabilistic versus probabilistic manner (Cramer, 2003). We illustrate this by constructing PSHA maps with a method that simply multiplies the PSHA for a hard rock site by the amplification factor appropriate for the site's ground motion level. This is approximately the method that Toro and Silva (2001) used before the development of the probabilistic methodology (Cramer, 2003). The site B/C response must be removed from the USGS PSHA maps before multiplication, which we approximate by division by the factors given in the work of Frankel et al. (1996). While this method confirms the same patterns of amplification, we point out significant differences from the completely probabilistic calculation. All acceleration levels using the simplified approach are slightly higher in the completely probabilistic approach.

A primary objective of this research with the new methodology was to provide input to the Indiana Department of Transportation (INDOT) for estimating the number of counties that will be affected by the proposed Recommended Load-and-Resistance-Factor Design (LRFD) Guidelines for the Seismic Design of Highway Bridges (ATC/MCEER, 2003). This document is currently under consideration by the American Association of State Highway and Transportation Officials, of which the INDOT is a member. In these guidelines, the seismic hazard level is taken as higher of the spectral acceleration with site amplification at 0.2 seconds and 1-second periods, as described in Tables 3 and 4 (ATC/MCEER, 2003). We have created a set of thematic maps that shows the maximum seismic hazard level for each county based

←

Table 3. *Spectral response amplification factors at 5-Hz ($S_s$) and at 1-Hz ($S_1$), from ATC/MCEER (2003). "a" indicates that site-specific evaluation is required.*

| | Mapped Spectral Response Acceleration Amplification Factor ($F_a$) at Short Periods | | | | |
|---|---|---|---|---|---|
| Site class | $S_s$ = 0.25 g | $S_s$ = 0.50 g | $S_s$ = 0.75 g | $S_s$ = 1.00 g | $S_s \geq$ 1.25 g |
| A | 0.8 | 0.8 | 0.8 | 0.8 | 0.8 |
| B | 1.0 | 1.0 | 1.0 | 1.0 | 1.0 |
| C | 1.2 | 1.2 | 1.1 | 1.0 | 1.0 |
| D | 1.6 | 1.4 | 1.2 | 1.1 | 1.0 |
| E | 2.5 | 1.7 | 1.2 | 0.9 | 0.9 |
| F | a | a | a | a | a |

| | Mapped Spectral Response Acceleration Amplification Factor ($F_v$) at 1-Second Periods | | | | |
|---|---|---|---|---|---|
| Site class | $S_1$ = 0.1 g | $S_1$ = 0.2 g | $S_1$ = 0.3 g | $S_1$ = 0.4 g | $S_1 \geq$ 0.5 g |
| A | 0.8 | 0.8 | 0.8 | 0.8 | 0.8 |
| B | 1.0 | 1.0 | 1.0 | 1.0 | 1.0 |
| C | 1.7 | 1.6 | 1.5 | 1.4 | 1.3 |
| D | 2.4 | 2.0 | 1.8 | 1.6 | 1.5 |
| E | 3.5 | 3.2 | 2.8 | 2.4 | 2.4 |
| F | a | a | a | a | a |

on several assumptions. In these maps the maximum acceleration level at 2 percent probability of exceedance is found in each county, then the corresponding seismic hazard level from Table 4 is found. The maximum of the values for the 1-Hz and 5-Hz seismic hazard levels is taken as the final seismic hazard level in the map. The first map is the original USGS 2002 PSHA with B/C site conditions (Figure 11a), the second is the USGS 2002 PSHA map with D site conditions (Figure 11b), the third is the USGS 2002 PSHA map with a simple multiplication by the site amplification factor calculated from the geology-based velocity model (Figure 11c), and the fourth map is the completely probabilistic site effects calculation (d). With most of the counties in Indiana having NEHRP Class D or Class E NEHRP classifications (Bauer et al., 2001), there is a great

Table 4. *Seismic hazard levels defined in table 3.10.3.1 of ATC/MCEER (2003). Fa and Fv are site coefficients described in Article 3.10.2.2.3 of ATC/MCEER (2003).*

| Seismic Hazard Level | Value of $FvS_1$ ($S_1$ = 1-Hz Spectral Acceleration) | Value of $FaS_s$ ($S_s$ = 5-Hz Spectral Acceleration) |
|---|---|---|
| I | $FvS_1 \leq 0.15$ | $FaS_s \leq 0.15$ |
| II | $0.15 < FvS_1 \leq 0.25$ | $0.15 < FaS_s \leq 0.35$ |
| III | $0.25 < FvS_1 \leq 0.40$ | $0.35 < FaS_s \leq 0.60$ |
| IV | $0.40 < FvS_1$ | $0.60 < FaS_s$ |

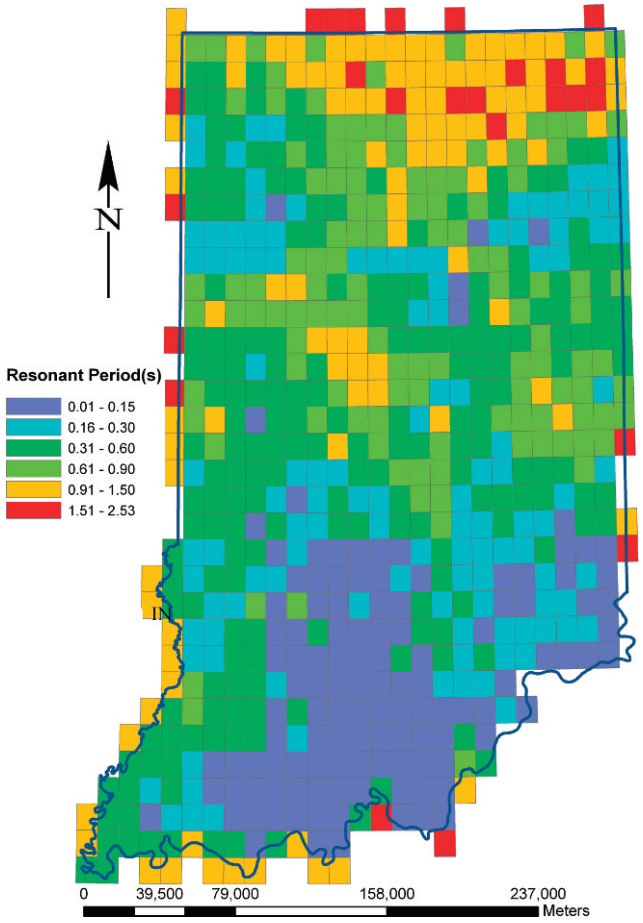


Figure 12. Map showing resonant period of the unconsolidated soil layer, given the shear wave velocity and thickness, calculated as $T$ (period) = $4h/V_s$.

impact in applying the amplification factors in the recommended LRFD guidelines. This can be seen by comparing the seismic hazard levels from the USGS 2002 map (Figure 13a) with the USGS 2002 map with Class D site effects (Figure 13b). In particular, there is an increase in the number of counties at seismic hazard level IV (from 5 to 11 counties), and all counties at the lowest seismic hazard level I move to seismic hazard level II.

Estimating site amplifications with a probabilistic method should give the most accurate results. There are differences between the number of counties affected using a simplified site effect multiplication factor (Figure 13c) and the probabilistic method (Figure 13d), even though the input geology-based velocity model is the same.

Using the probabilistic method, even with an approximate geology-based shear wave velocity model, actually reduces the number of counties at seismic hazard level IV, compared to the 2002 USGS maps both with and without Class D site effects. This

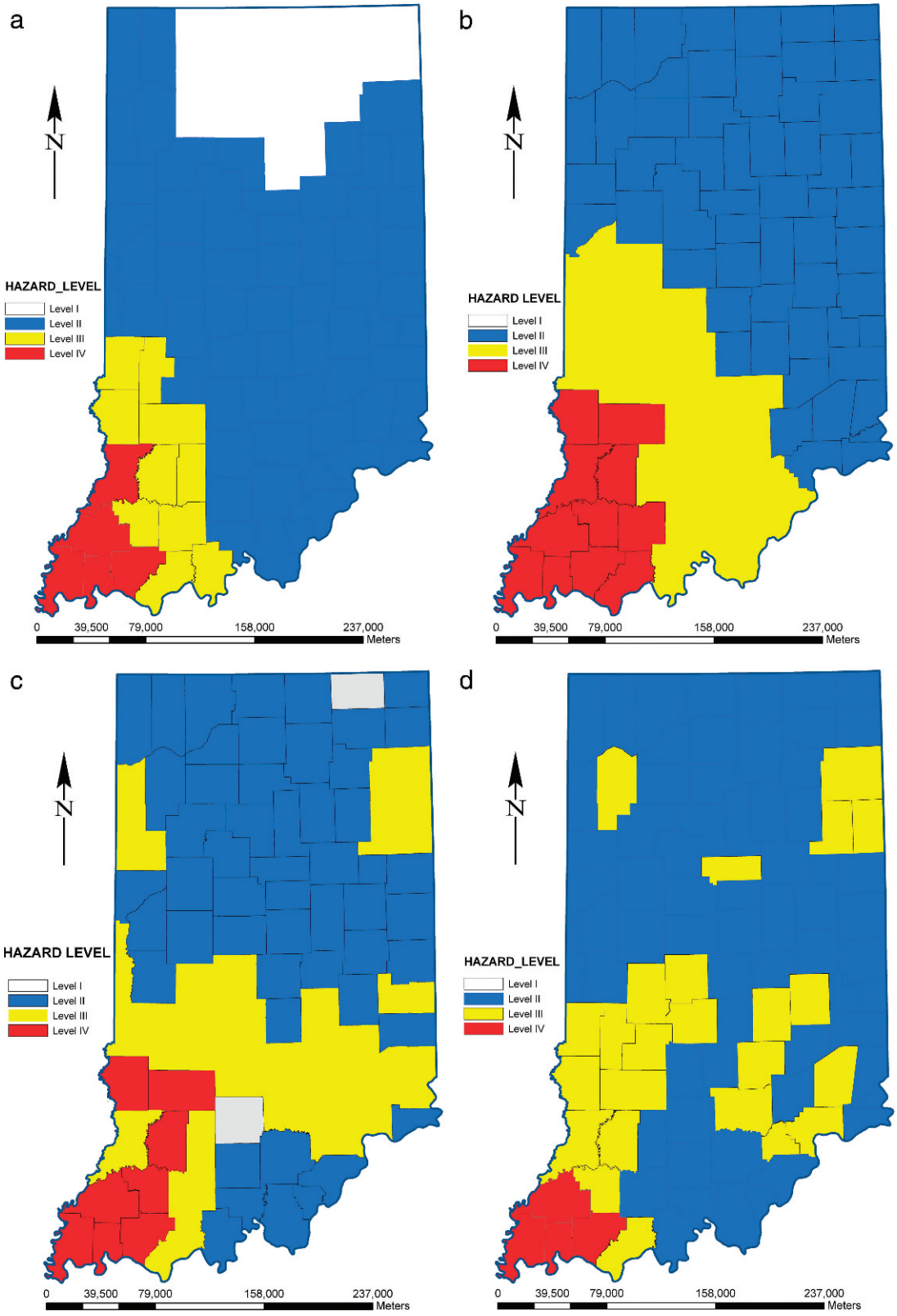


Figure 13. Map of the estimated maximum seismic hazard level (ATC/MCEER, 2003) for each county for the (a) standard 2002 USGS PSHA maps with B/C site conditions, (b) 2002 USGS PSHA maps with D site conditions, (c) 2002 PSHA maps with multiplication by site response factor, and (d) PSHA maps with probabilistic site response. Seismic hazard level is determined from the maximum of 1-Hz and 5-Hz seismic hazard levels.

can be seen by comparing the probabilistic site effect map (Figure 13d) with the two versions of the USGS 2002 maps (Figure 13a,b). Most importantly, the counties at seismic hazard level III are not the same between the Class D site effect method and the probabilistic site effect map.

Based on these preliminary maps with probabilistic site effects and the criteria defined in the Recommended LRFD Guidelines for the Seismic Design of Highway Bridges, there are four Indiana counties at seismic hazard level IV, 24 counties at seismic hazard level III, and 64 counties at seismic hazard level II; there are no counties at seismic hazard level I. In comparison, using the USGS 2002 maps without considering site effects (using the B/C site classification), there are five counties at seismic hazard level IV, 10 counties at seismic hazard level III, 62 counties at seismic hazard level II, and 15 counties at seismic hazard level I. These comparisons are summarized in Table 5. Future versions of PSHA maps with probabilistically incorporated site effects should be planned that will create and use a database with higher-resolution information on shear wave velocity structure and which address some of the approximations that were necessary given the scope of the current project.

Table 5. *Number of counties estimated at each seismic hazard level for different methodologies.*

| Maximum of 5-Hz and 1-Hz Seismic Hazard Level | No. of Counties for 2002 USGS Map with Default B/C Site Effects | No. of Counties for 2002 USGS with Class D Site Effects | No. of Counties for Map Including Probabilistic Site Effects |
|---|---|---|---|
| I | 15 | 0 | 0 |
| II | 62 | 57 | 64 |
| III | 20 | 24 | 24 |
| IV | 5 | 11 | 4 |

## DISCUSSION

Our calculations of probabilistic seismic hazard with probabilistic incorporation of site effects are intended to provide a preliminary understanding of the way in which gross features of the geologic structure of Indiana may potentially affect expected acceleration levels in the state. While the oversimplified input model limits the resolution of the product to the quadrangle scale, it is the first visual product of state-wide PSHA available at that scale. As a starting point it achieves its objectives; however, we note below the most significant of the improvements that should be implemented in the future.

### Depth Dependence of Surficial Velocities

We have assumed that the velocities assigned at the surface continue to bedrock depths, where it is more reasonable to assume that velocities increase with effective stress. The observed correlation between the average velocity and the depth of the second soil layer indicates that this type of relationship is reasonable. In this sense the maps are conservative, in that they represent the upper limit on the amplification. Future versions of the maps would be improved by incorporating the true depth dependence of seismic velocity or at least a theoretical increase in velocity with depth.

### Characterization of Surficial Velocity by Lithology

The lithologic classification that we chose was limited because of the number of shear wave profile measurements available. In this case we used approximately 50 measurements. The number of observations should be increased by collecting more data or by including other types of compiled data, such as blow count data and cone penetration test data. It is necessary either to sample the shear wave velocity sufficiently densely across the state or to make more measurements to provide better characterization of each lithology. This latter approach would permit a more detailed classification (more units) that would help give a better spatial representation of the shear wave velocity model. The nature of the glacial tills, for example, which cover so much of Indiana, is such that their material properties are highly variable. Future versions of the maps, then, would be improved in spatial resolution.

### Discretization and Aliasing Issues

For simplicity we sampled the surficial geologic maps at the quadrangle center points to determine the properties of the site used in the site response calculation. Therefore, smaller-scale features such as river valleys, which are expected to provide significantly higher amplification, are not sampled properly. The uncertainties associated with each site velocity could be improved to take into account the probability of sampling each type of lithology found in the quadrangle, for example. This would provide a better spatial smoothness to the output maps.

## CONCLUSIONS

We have reproduced the probabilistic seismic hazard calculation following the USGS methodology for the state of Indiana and have provided details for the shaking level on each county of the state. The original seismic hazard maps (Frankel et al., 1996,

2002) were constructed assuming firm-rock sites. We have assessed the hazard on a county-by-county basis, taking into account that the local soil conditions can produce amplification of shaking in regions relative to firm-rock sites. We have used a low-resolution geology-based shear wave velocity model with characteristics specific to the state of Indiana as input to a completely probabilistic calculation, with site effects incorporated into the PSHA. Thus, we produced maps with amplification and de-amplification relative to the 2002 USGS PSHA maps, with quadrangle-scale resolution, which is limited by the density of information from the input velocity model. For the 1-Hz ground motion with 2 percent probability of being exceeded in 50 years, the maximum difference between the standard NEHRP B/C site and the probabilistic site effect calculation is over a factor of 2. This occurs in the central and central-northern parts of the state, where the surficial units of glacial tills are particularly thick. For the 5-Hz ground motion with 2 percent probability of being exceeded in 50 years, the maximum difference between the standard NEHRP B/C site and the probabilistic site effect calculation is over a factor of 2.5 in the northeast of the state as a result of sediments of intermediate thickness with slow velocities. The 5-Hz ground motion was de-amplified somewhat in the extreme southwest part of the state because of the non-linear response of the soils at high ground motions. Fifty percent lower amplitudes are also noted for a good portion of the south-central part of the state because of the surficial bedrock units present. These preliminary results are useful, since they give a first-order estimate that illustrates the potential effect of geology and, in particular, the spatial patterns of amplification. They are demonstration maps that serve as a proof of concept for the probabilistic site effect methodology.

Based on these preliminary maps with probabilistic site effects and the criteria defined in the Recommended LRFD Guidelines for the Seismic Design of Highway Bridges, there are four Indiana counties at seismic hazard level IV, 24 counties at seismic hazard level III, and 64 counties at seismic hazard level II; there are no counties at seismic hazard level I. In comparison, the USGS 2002 maps with simple consideration of D classification site effects (most of Indiana has D or E site classifications) show 11 counties at seismic hazard level IV, 24 counties at seismic hazard level III, 57 counties at seismic hazard level II, and no counties at seismic hazard level I. In this case, a more precise methodology actually reduces the number of counties at the highest seismic hazard level. Future versions of PSHA maps with site effects should be planned that will use a database with higher-resolution information on shear wave velocity structure and that will address some of the approximations that were necessary given the scope of the current project. These future maps will provide information at the level necessary for planning and budgeting, though site-specific studies will still be needed for engineering.

## ACKNOWLEDGMENTS

This work was supported by Joint Transportation Research Program grant SPR-2812, ''Analysis of Seismic Hazard Assessments for Indiana,'' administered by the Indiana Department of Transportation and Purdue University. The authors would like to thank Vince Drnevich for discussions on implementing the soil classification–based shear wave velocity relation. The authors thank Brent Foshee for help in collecting borehole shear wave velocity data and the Indiana Geological Survey for providing access to the many data sets used in this work. The authors thank the Indiana Earthquake Hazard Preparedness and Response Committee for input and discussions regarding the work.

## REFERENCES

ATC/MCEER, 2003, *Recommended LRFD Guidelines for the Seismic Design of Highway Bridges, Part I: Specifications and Part II: Commentary and Appendices*: MCEER-03-SP03, MCEER, Buffalo, NY.

Atkinson, G. and Boore, D., 1995, Ground-motion relations for eastern North America: *Bulletin Seismological Society America*, Vol. 85, No. 1, pp. 17–30.

Bauer, R. A., 1997, *Compilation of Databases and Map Preparation for Regional and Local Seismic Zonation Studies in the CUSEC Region: Collaborative Research—Organization of CUSEC State Geologists with Assistance from USGS and Administrative Support from CUSEC*: Report 1434-HQ-97-GR-03150, Illinois State Geological Survey, Champaign, IL, 20 p.

Bauer, R. A.; Kiefer, J.; and Hester, N., 2001, Soil amplification maps for estimating earthquake ground motions in the Central US: *Engineering Geologist*, Vol. 62, No. 1–3, pp. 7–17.

Bechtel-Jacobs, 2002, *Paducah Gaseous Diffusion Plant: Re-evaluation of Site-Specific Soil Column Effects on Ground Motion*: Report BJC/PAD-356, Department of Energy.

Braile, L. W.; Keller, G. R.; Hinze, W. J.; and Lidiak, E. G., 1982, An ancient rift complex and its relation to contemporary seismicity in the New Madrid seismic zone: *Tectonics*, Vol. 1, No. 2, pp. 225–237.

Building Seismic Safety Council (BSSC), 2004, *National Earthquake Hazards Reduction Program Recommended Provisions for Seismic Regulations for New Buildings and Other Structures (FEMA 450), Part 1: Provisions*: Building Seismic Safety Council, Washington, DC, 356 p.

Campbell, K. W., 2003, Prediction of strong ground motion using the hybrid empirical method and its use in the development of ground-motion (attenuation) relations in eastern north

America: *Bulletin Seismological Society America*, Vol. 93, No. 3, pp. 1012–1033.

Cornell, C. A., 1968, Engineering seismic risk analysis: *Bulletin Seismological Society America*, Vol. 58, No. 5, pp. 1583–1606.

Cramer, C., 2005, Erratum: Site-specific seismic hazard analysis that is completely probabilistic: *Bulletin Seismological Society America*, Vol. 95, No. 5, p. 2026.

Cramer, C. H., 2003, Site specific seismic hazard analysis that is completely probabilistic: *Bulletin Seismological Society America*, Vol. 93, No. 4, pp. 1841–1846.

Eggert, D. L.; Samuelson, A. C.; Bray, J. D.; Chang, C. W.; Eckhoff, W. R.; Kayabali, K.; McClees, E. J.; West, T. R.; Woodfield, M. C.; and Zheng, B., 1994, *Final Report to the City of Evansville: Shear-Wave and Earthquake Hazard Mapping of Evansville, Indiana*: Open File Studies, OFS94-19, Indiana Geological Survey, Bloomington, IN, 17 p.

Eggert, D. L.; Woodfield, M. C.; Bleuer, N. K.; and Hartke, E. J., 1997, *Geologic Terrain Map of the Evansville Region, Indiana*: Open File Studies, OFS97-16, Indiana Geological Survey, Bloomington, IN.

Electric Power Research Institute (EPRI), 1993, *Guidelines for Determining Design Basis Ground Motions,* Vols. 1–5: Report TR-102293, Electric Power Research Institute, Palo Alto, CA.

Federal Emergency Management Agency (FEMA), FEMA-222A, 1994, *NEHRP Recommended Provisions for the Development of Seismic Regulations for New Buildings, 1994 Edition, Part 1—Provisions*: Federal Emergency Management Agency, 290 p.

Frankel, A.; Mueller, C.; Barnhard, T.; Perkins, D.; Leyendecker, E. V.; Dickman, N.; Hanson, S.; and Hopper, M., 1996, *National Seismic Hazard Maps*: Documentation June 1996: U.S. Geological Survey Open File Report 96-532, 110 p.

Frankel, A.; Petersen, M.; Mueller, C.; Haller, K.; Wheeler, R.; Leyendecker, E. V.; Wesson, R.; Harmsen, S.; Cramer, C.; Perkins, D.; and Rukstales, K., 2002, *Documentation for the 2002 Update of the National Seismic Hazard Maps*: U.S. Geological Survey Open File Report 02-420, 33 p.

Gomberg, J.; Waldron, B.; Schweig, E.; Hwang, H.; Webbers, A.; Vanarsdale, R.; Tucker, K.; Williams, R.; Street, R.; Mayne, P.; Stephenson, W.; Odum, J.; Cramer, C.; Updike, R.; Hutson, S.; and Bradle, M., 2003, Lithology and shear-wave velocity in Memphis, Tennessee: *Bulletin Seismological Society America*, Vol. 93, No. 3, pp. 986–997.

Gray, H. H., 1983, *Map of Indiana Showing Thickness of Unconsolidated Deposits*: Miscellaneous Map 37, Indiana Geological Survey, 1:500,000, Bloomington, IN.

Gray, H. H., 1989, *Quaternary Geologic Map of Indiana*: Indiana Geological Survey Miscellaneous Map 49, 1:500,000, Bloomington, IN.

Green, R. A.; Obermeier, S. F.; and Olson, S. M., 2005, Engineering geologic and geotechnical analysis of paleoseismic shaking using liquefaction effects: Field examples: *Engineering Geologist*, Vol. 76, pp. 263–293.

Hamilton, E. L., 1979, Vp/Vs and Poisson's ratios in marine sediments and rocks: *Journal Acoustical Society America*, Vol. 66, No. 4, pp. 1093–1101.

Hill, J. R. and Foshee, B. D., 2008, *A Preliminary Guide to the Responses of Geologic Materials in Indiana to Seismically Induced Ground Shaking*: IGS Report of Progress RP35, Indiana Geological Survey, Bloomington, IN, 39 p.

Hough, S. E.; Armbruster, J. G.; Seeber, L.; and Hough, J. F., 2000, On the Modified Mercalli Intensities and magnitudes of the 1811–1812 New Madrid earthquakes: *Journal Geophysical Research–Solid Earth*, Vol. 105, No. B10, pp. 23839–23864.

Idriss, I. M. and Sun, J. I., 1992, *User's Manual for SHAKE91*: Center for Geotechnical Modeling, Department of Civil and Environmental Engineering, University of California, Davis, Davis, CA.

Johnston, A. C., 1996, Seismic moment assessment of earthquakes in stable continental regions: II. New Madrid 1811–1812, Charleston 1886 and Lisbon 1755: *Geophysical Journal International*, Vol. 126, No. 2, pp. 314–344.

Johnston, A. C. and Schweig, E. S., 1996, The enigma of the New Madrid earthquakes of 1811–1812: *Annual Reviews Earth Planetary Science*, Vol. 24, pp. 339–384.

Kelson, K. I.; Simpson, G. D.; Vanarsdale, R. B.; Haraden, C. C.; and Lettis, W. R., 1996, Multiple Late Holocene earthquakes along the Reelfoot fault, central New Madrid seismic zone: *Journal Geophysical Research–Solid Earth*, Vol. 101, No. B3, pp. 6151–6170.

Lee, R. C., 2000, *A Methodology to Integrate Site Response into Probabilistic Seismic Hazard Analysis*: Site Geotechnical Services, Savannah River Site.

McGuire, R. K., 2004, *Seismic Hazard and Risk Analysis*: Earthquake Engineering Research Institute MNO-10, 221 p.

Olson, S. M.; Green, R. A.; and Obermeier, S. F., 2005, Revised magnitude-bound relation for the Wabash Valley seismic zone of the central United States: *Seismological Research Letters*, Vol. 76, No. 6, pp. 756–771.

Pacific Earthquake Engineering Research Center, 2009, *PEER Strong Motion Database*.

Reiter, L., 1990, *Earthquake Hazard Analysis: Issues and Insights*: Columbia University Press, New York, 233 p.

Rockaway, T. D., 1997, *Spatial Assessment of Earthquake Induced Geotechnical Hazards*: Ph.D. Thesis, Georgia Institute of Technology, Atlanta, GA, 418 p.

Rudman, A. J.; Biggs, M. E.; Blakely, R. F.; and Whaley, J. F., 1973, Statistical studies of Indiana bedrock velocities: Mapping applications: *Indiana Academy Science*, Vol. 83, pp. 284–290.

Seeber, L. and Armbruster, J. G., 1991, *The NCEER-91 Earthquake Catalog: Improved Intensity-Based Magnitudes and Recurrence Relations for U.S. Earthquakes East of New Madrid*: NCEER-91-0021, National Center for Earthquake Engineering Research.

Sipkin, S. A.; Person, W. J.; and Presgrave, B. W., 2000, Earthquake bulletins and catalogs at the USGS National Earthquake Information Center: *IRIS Newsletter*, Vol. 2, No. 1, pp. 2–4.

Somerville, P. G.; Collins, N.; Abrahamson, N.; Graves, R.; and Saikia, C., 2001, *Ground Motion Attenuation Relations for the Central and Eastern United States*: Final Report for U.S. Geological Survey Grant No. 99HQGR0098, 38 p.

Street, R.; Woolery, E. W.; Wang, Z. M.; and Harris, J. B., 2001, NEHRP soil classifications for estimating site-dependent seismic coefficients in the Upper Mississippi Embayment: *Engineering Geologist*, Vol. 62, No. 1–3, pp. 123–135.

Toro, G. R.; Abrahamson, N. A.; and Schneider, J. F., 1997, Model of strong ground motions from earthquakes in central and eastern North America: Best estimates and uncertainties: *Seismological Research Letters*, Vol. 68, No. 1, pp. 41–57.

Toro, G. R. and Silva, W. J., 2001, *Scenario Earthquakes for St. Louis, MO, and Memphis, TN, and Seismic Hazard Maps for the Central United States Region Including the Effect of Site Conditions*: Final Technical Report.

Tuttle, M.; Schweig, E. S.; Sims, J. D.; Lafferty, R. H.; Wolf, L. W.; and Haynes, M. L., 2002, The earthquake potential of the New Madrid Seismic Zone: *Bulletin Seismological Society America*, Vol. 92, pp. 2080–2089.

Tuttle, M. P.; Collier, J.; Wolf, L. W.; and Lafferty, R. H., 1999, New evidence for a large earthquake in the New

Madrid seismic zone between AD 1400 and 1670: *Geology*, Vol. 27, No. 9, pp. 771–774.

Tuttle, M. P. and Schweig, E. S., 1995, Archaeological and pedological evidence for large prehistoric earthquakes in the New-Madrid seismic zone, central United States: *Geology*, Vol. 23, No. 3, pp. 253–256.

Vucetic, M. and Dobry, R., 1991, Effect of soil plasticity on cyclic response: *Journal Geotechnical Engineering*, Vol. 117, pp. 89–107.

Whaley, J. F.; Blakely, R. F.; Like, K. K.; and James, C. L., 2002, *Seismic Refraction Data for Indiana (Indiana Geological Survey, Point Shapefile)*: Indiana Geological Survey, Bloomington, IN.

Wheeler, R. L. and Cramer, C. H., 2002, Updated seismic hazard in the southern Illinois Basin: Geological and geophysical foundations for use in the 2002 USGS National Seismic Hazard Maps: *Seismological Research Letters*, Vol. 73, No. 5, pp. 776–791.

Zoback, M. D. and Zoback, M. L., 1991, Tectonic stress field of North America and relative plate motions. In Slemmons, D. B.; Engdahl, E. R.; Zoback, M. D.; and Blackwell, D. D. (Editors), *Neotectonics of North America, GSA, Decade Map*: Geological Society of America, Boulder, CO, pp. 339–366.

Zoback, M. L., 1992, Stress-field constraints on intraplate seismicity in eastern North America: *Journal Geophysical Research–Solid Earth*, Vol. 97, No. B8, pp. 11761–11782.